Clinical Trial/Experimental Study

Medicine®

OPEN

Effects of flavopiridol on critical regulation pathways of CD133^{high}/CD44^{high} lung cancer stem cells

Vildan Bozok Cetintas, PhD[a], Eda Acikgoz, MSc[b,c,*], Gurkan Yigitturk, MSc[c], Kenan Demir, MD[c], Gulperi Oktem, MD[c], Burçin Tezcanli Kaymaz, PhD[a], Fatih Oltulu, MD[c], Huseyin Aktug, MD[c]

Abstract

Background: Flavopiridol a semisynthetic flavone that inhibits cyclin-dependent kinases (CDKs) and has growth-inhibitory activity and induces a blockade of cell-cycle progression at G1-phase and apoptosis in numerous human tumor cell lines and is currently under investigation in phase II clinical trials. Cancer stem cells (CSCs) are comprised of subpopulation of cells in tumors that have been proposed to be responsible for recurrence and resistance to chemotherapy. The aim of the present study was to investigate the effects of flavopiridol in cancer stem cell cytoskeleton, cell adhesion, and epithelial to mesenchymal transition in CSCs.

Methods: The cells were treated with flavopiridol to determine the inhibitory effect. Cell viability and proliferation were determined by using the WST-1 assay. Caspase activity and immunofluorescence analyses were performed for the evaluation of apoptosis, cell cytoskeleton, and epithelial-mesenchymal transition (EMT) markers. The effects of flavopiridol on the cell cycle were also evaluated. Flow cytometric analysis was used to detect the percentages of CSCs subpopulation. We analyzed the gene expression patterns to predict cell cycle and cell cytoskeleton in CSCs by RT-PCR.

Results: Flavopiridol-induced cytotoxicity and apoptosis at the IC_{50} dose, resulting in a significant increase expression of caspases activity. Cell cycle analyses revealed that flavopiridol induces G1 phase cell cycle arrest. Flavopiridol significantly decreased the mRNA expressions of the genes that regulate the cell cytoskeleton and cell cycle components and cell motility in CSCs.

Conclusion: Our results suggest that Flavopiridol has activity against lung CSCs and may be effective chemotherapeutic molecule for lung cancer treatment.

Abbreviations: Actb = Beta-actin, ALDH1 = aldehyde dehydrogenase1, ankyrin repeat and PH domain-1, Arap1 = ArfGAP with RhoGAP domain, Bcl2 = B-cell CLL/lymphoma-2, CDC25A = cell division cycle 25A, CDKN1A (p21) = cyclin-dependent kinase inhibitor 1A, CDKs = cyclin-dependent kinases, CHEK2 = checkpoint kinase 2, CSCs = cancer stem cells, DMSO = dimethyl sulfoxide, EMT = epithelial-mesenchymal transition, FACS = Fluorescence-activated cell sorting, Fnbp1l = Formin binding protein-1-like, Gapdh = Glyceraldehyde-3-phosphate dehydrogenase, Krt = keratin, Limk1 = LIM domain kinase-1, PAK4 = p21 (RAC1) activated kinase 4, PI = Propidium iodide, Rn18s = 18S ribosomal RNA, *SqCLCs* = *squamous cell lung carcinomas*, Ssh1 = slingshot protein phosphatase-1.

Keywords: apoptosis, cell cytoskeleton, EMT, flavopiridol, lung cancer, stem cell

1. Introduction

Lung cancer is among the leading causes of cancer deaths in the United States and in the world.[1] There are 2 main types of lung cancer as nonsmall cell lung cancer and small cell lung cancer. Nonsmall cell lung cancer can be divided into 3 major histological subtypes: squamous-cell carcinoma, adenocarcinoma, and large-cell lung cancer. The molecular heterogeneity of the tumor is the major cause of the dramatic difference in response to treatment in patients with nonsmall cell lung cancer.[2]

Tumors contain a small subpopulation of cells called cancer stem cells (CSCs) within tumors are responsible for tumor initiation, drug resistance, metastasis, and relaps of cancers. The presence of CSCs was determined in breast cancers, brain tumors, colon cancers, and lung cancers.[3,4] CSCs are resistant to chemotherapy and radiotherapy. Conventional therapies kill the bulk of tumor, may ultimately fail to specifically target CSCs. Thus, specifically targeting and eliminating CSCs may be an alternative for developing new therapeutic approaches to treating cancer.[5]

Flavopiridol is a potent inhibitor of CDKs. Flavopiridol has antitumor activity activity against various types of cancer.[6] Flavopiridol has strong activity on cyclin-dependent kinases whereas little activity on receptor tyrosine kinases and signal transducing kinases. More specifically, flavopiridol acts on tumor cells through cytotoxic activity, supporting cell cycle arrest and apopotosis.[7]

EMT plays a central role in cancer progression, metastatic spread, drug resistance, and is involved in the acquisition of

Editor: Maohua Xie.

The authors have no funding and conflicts of interest to disclose.

[a] Department of Medical Biology, Ege University Faculty of Medicine, Izmir, [b] Department of Histology and Embryology, Yuzuncu Yil University Faculty of Medicine, Van, [c] Department of Histology and Embryology, Ege University Faculty of Medicine, Izmir, Turkey.

[*] Correspondence: Eda Acikgoz, Yuzuncu Yil University Faculty of Medicine, Department of Histology and Embryology, Ege University Faculty of Medicine, Izmir, Turkey (e-mail: acikgozedaa@gmail.com).

Medicine (2016) 95:43(e5150)

Received: 3 March 2016 / Received in final form: 20 September 2016 / Accepted: 25 September 2016

http://dx.doi.org/10.1097/MD.0000000000005150

stemness phenotype of many tumors, including breast cancer, prostate cancer, pancreatic cancer, and hepatoma.[8] However, the role of EMT in lung cancer is still limited. Apical-basal polarity is a distinctive feature of epithelial cells characterized by the formation of specialized membrane regions and is also thought to prevent cell proliferation and tumor formation.[9] Cell polarity plays an important role in many biological process, such as cell division, cell adhesion, migration, and EMT. Loss of functional activity of polarity may lead to cancer development and invasiveness.[10]

In the cells that the damage cannot be repaired, cell cycle arrest and repair mechanism may induce a cell-specific apoptotic response. The failure that occur throughout this process can lead to tumor development.[11] Apoptotic signaling pathways are deregulated in lung CSCs CSCs express high levels of antiapoptosis proteins.[12] Flavopiridol can induce cytotoxic effects by cell cycle arrest at G1 and G2 phases though inhibition of Cdk2, Cdk4, and Cdk1 and induction of apoptosis in various human cancers.

The purpose of this study was to investigate the effect of flavopiridol on cellular proliferation, cell cycle distribution, polarity, and apoptosis. Another important objective of the study was to identify the behavioral model of cell polarity and motility components in lung CSCs as well as to manifest how flavopridol affects this process.

2. Material and methods

2.1. Cell culturing conditions and reagents

Lung squamous carcinoma cells (SqCLCs, KLN205) were obtained from American Type Culture Collection (ATCC, Manassas, VA). Cells were cultured in Dulbecco's Modified Eagle's Medium (DMEM, Bio. Ind., Kibbutz BeitHaemek, Israel) containing 10% (v/v) heat-inactivated fetal calf serum (Bio. Ind.), 100 units of penicillin–streptomycin/mL (Bio. Ind.), 1% L-glutamine (Bio. Ind.) at 37 °C in humidified atmosphere of 5% CO_2. Flavopiridol was obtained from Sigma Aldrich (St Louis, MO) and dissolved in dimethyl sulfoxide (DMSO). The antibodies used were anti-HSP90β (1:100 diluted; bs-0135R, Bioss, China), anti-E-cadherin (1:100 diluted; sc-7870, Santa Cruz Biotechnology, Inc., Santa Cruz, CA), anti-occludin (1:100 diluted; sc-271842, Santa Cruz Biotechnology, Inc., Santa Cruz, CA), antiactin (1:100 diluted; sc-8432, Santa Cruz Biotechnology, Inc., Santa Cruz, CA) antitubulin (1:100 diluted; ab6161, Abcam, Cambridge, MA) anticytokeratin-2 (1:100 diluted; ab174703, Abcam, Cambridge, MA) anticaspase-3 (1:100 diluted; bs-0081R, Bioss, China), anticaspase-8 (1:100 diluted; bs-6463R,Bioss, China), anticaspase-9 (1:100 diluted; bs-3082R, Bioss, China), and goat antirabbit immunoglobulin G-fluorescein isothiocyanate (FITC) (1:100 diluted; ab98692, Abcam, Cambridge, MA) and rabbit antimouse immunoglobulin G-fluorescein isothiocyanate (FITC) (1:100 diluted; bs-0296R, Bioss, China).

This study was conducted using a commercially available lung squamous carcinoma cells (SqCLCs, KLN205); no in vivo experiments on animals or humans were performed and therefore approval from an ethics committee was not necessary.

2.2. Fluorescence-activated cell sorting (FACS)

Flow cytometric analysis was used to detect $CD133^{high}/CD44^{high}$ cell population. The cells were analyzed by FACS after reaching the logarithmic proliferation phase. For FACS (FACSAria; BD Biosciences, San Jose, CA), the cells were detached using nonenzymatic cell dissociation solution (Sigma-Aldrich) and $\sim 5 \times 10^4$ cells were incubated with an antibody (diluted 1:100 in FACS wash with 0.5% bovine serum albumin; 2 mM NaN3 and 5 mMEDTA) for 15 minutes at 4°C. An isotype and concentration-matched phycoerythrin (PE)-labeled control antibody was used and the samples were labeled with PE-labeled CD133/1 and FITC-labeled CD44. After 3 to 5 minutes, the cells were washed with the FACS wash, and subsequently the cells were resuspended. The cells were organized into a $CD133^{high}/CD44^{high}$ subpopulation to become CSCs.

2.3. Cytotoxicity assay

Cell viability and proliferation of untreated controls and flavopiridol treated cells were determined by using the WST-1 assay (Roche Applied Science, Mannheim, Germany). CSCs were placed into 96-well plate at a density of 3×10^4 cells in 100 μL medium per well. Then, cells were treated with increasing doses of flavopiridol for 48 hours. After having performed the proliferation assay, absorbance of each sample was measured spectrophotometrically at 450 nm with an ELISA reader (Thermo, Vantaa, Finland).

2.4. Caspase activity assay

Caspase-3, -8, and -9 activities were analyzed using Colorimetric Assay Kits (Biovision Research Products, Mountain View, CA). 1×10^6 cells were collected and resuspended in chilled lysis buffer. After centrifugation the supernatant was aliquoted and caspase activities were measured. Samples were incubated at 37°C for 2 hours with reaction buffer and substrate. Finally, absorbance was measured spectrophotometrically at 405 nm with an ELISA reader.

2.5. Cell cycle analysis

Cycle TEST™ PLUS DNA reagent Kit (Becton Dickinson) was used for cell cycle analyses. 1×10^6 cells were collected and trypsinized with solution A to digestion of cell membranes and cytoskeletons. After inhibition of trypsin activation, propidium iodide (PI) containing solution C was added. Cells were incubated for 10 minutes in the dark on ice and analysed on the flow cytometer (BD Accuri C6 Flow Cytometer).

2.6. Determination of differentially expressed genes by real-time ready array

Total RNA was isolated from untreated and flavopiridol treated $CD133^{high}/CD44^{high}$ CSCs using the MagNA Pure LC RNA Isolation Kit (Roche Applied Science, Mannheim, Germany). 10 μg of total RNA was reverse-transcribed with the Transcriptor High Fidelity cDNA Synthesis Kit (Roche Applied Science). A real-time ready custom array panel was designed for the quantification of differently expressed gene expressions by real-time PCR using the LightCycler 480 instrument. Relative quantification of each sample with Glyceraldehyde-3-phosphate dehydrogenase (Gapdh), Beta-actin (Actb) and 18S ribosomal RNA (Rn18s) housekeeping genes were achieved by using the software of the instrument.

2.7. Immunofluorescence staining

$CD133^{high}/CD44^{high}$ lung CSCs were treated as indicated above and were harvested and fixed in 4% paraformaldehyde for 15 minutes. Subsequently, the cells were rendered permeable with 0.1% Triton X–100 for 10 minutes at room temperature, and blocked with

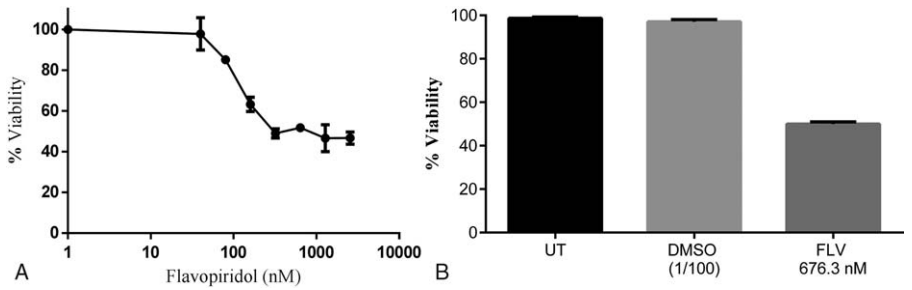

Figure 1. WST cytotoxicity assay results of flavopiridol and DMSO (A) $CD133^{high}/CD44^{high}$ lung CSCs treated with flavopiridol. Exponentially growing cells were incubated with flavopiridol at the 40, 80, 160, 320, 640, 1280, and 2560 nM concentrations for 48 h. Each concentration was studied as 3 replicates. The concentration of flavopiridol that inhibited cell growth at 50% (IC_{50}) was calculated as 676.3 nM at 48 h from cell viability inhibition curve. (B) Evaluation of the cytotoxicity effect of dimethyl sulfoxide (DMSO) at the used concentration in the experiments. CSCs = cancer stem cells, DMSO = dimethyl sulfoxide.

phosphate–buffered saline containing 5% bovine serum albumin for 1 hour. Following incubation with antibodies against caspase-3, caspase-8, caspase-9, e-cadherin, hsp90β, actin, tubulin, occludin, and cytokeratin-2 over night at 4 C, the CSCs were treated with FITC–conjugated secondary antibody for 1 hour at room temperature. The cells were counterstained with 4′,6–diamidino–2–phenylindole and assessed by a fluorescence microscope equipped with a camera (Olympus BX–51 and the Olympus C–5050 digital test).

2.8. Statistical analyses

Gene expression values were collected with both relative quantification and absolute quantification analyses of LightCycler 480 software. Relative quantification values which are normalized to the housekeeping genes (Actb, Gapdh and Rn18s) used for statistical analyses with CLC Main Workbench software. Log2 transformation was performed to the expression values and fold change values; FDR (False Discovery Rate) corrected *P* values were calculated. To confirm these, CT (cycle threshold) values from absolute quantification analysis used with RT^2 Profiler PCR Array Data Analysis version 3.5 (SABiosiciences). IC_{50} flavopiridol concentrations were calculated with the GraphPad Prism Software 5.01. All data are presented as mean ± standard deviation from 3 independent experiments. Statistical differences were evaluated using Student's *t*-test and considered significant at $P < 0.05$.

3. Results

3.1. Purity of $CD133^{high}/CD44^{high}$–sorted subpopulations and sorting rates

SqCLCs were separated with FACS as the $CD133^{high}/CD44^{high}$ population (sorted cells). The purity of the CSCs samples was tested with CD133 and CD44 antibodies. The sorting rate analysis and purity of the cells were evaluated sequentially and the rate was 94.7 ± 5.8% for the sorted cells. In order to confirm the flow cytometry analyses, the cells were re–evaluated following sorting and the analyses were repeated after 1 passage. The results showed that the cell purity following sorting was 85%. Immunofluorescence staining yielded a cell purity of >85% in all the samples.

3.2. Increasing cytotoxicity of $CD133^{high}/CD44^{high}$ lung CSCs with flavopiridol

In order to study the effects of flavopiridol on $CD133^{high}/CD44^{high}$ lung CSCs, cells were treated with increasing concentrations of flavopiridol (40, 80, 160, 320, 640, 1280, and 2560 nM). After 48 hours, viability was evaluated by WST cytotoxicity assay. Cell viability was taken as 100% in the control cells and 97%, 85%, 63%, 48%, 51%, and 46% viabilities were detected at the treatment groups, respectively (Fig. 1A). These results revealed that cell growth was inhibited by flavopiridol in a dose-dependent manner. According to the flavopiridol inhibition curve, IC_{50} dose was calculated as 676.3 nM for $CD133^{high}/CD44^{high}$ lung CSCs. When we tested the cytotoxicity effect of dimethyl sulfoxide (DMSO), no statistical difference in toxicity was observed between the control and 1/100 DMSO-treated groups (Fig. 1B).

3.3. Caspase-3, caspase-8, and caspase-9 modulate flavopiridol–associated apoptosis

To examine the apoptotic effects of flavopiridol, we analyzed caspase-3, caspase-8 and caspase-9 activities in $CD133^{high}/CD44^{high}$ lung CSCs. Caspase-3 and caspase-8 activities were increased to 95% and 70% respectively after flavopiridol treatment ($P = 0.0008$ and $P = 0.026$). Although caspase-9 activity slightly increased (39%) in the flavopiridol-treated cells, this increment was not statistically significant (Fig. 2).

3.4. Expression of caspases in $CD133^{high}/CD44^{high}$ lung CSCs

Flavopiridol treatment with an IC_{50} dose resulted in a significant increase in immunofluorescence staining of caspase-3, caspase-8, and caspase-9 when compared to the control ($P < 0.05$). No significant changes were observed in immunofluorescence staining of caspase-8 when compared to the control (Fig. 3).

3.5. Cell cycle regulation with flavopiridol treatment

The effects of flavopiridol on the cell cycle of the $CD133^{high}/CD44^{high}$ lung CSCs are shown in Fig. 4. Flow cytometry results showed that flavopiridol-induced cell cycle arrest in the G0/G1 phase after 48 hours of exposure to 676.3 nM flavopiridol. The fraction of CSCs in the G1 phase increased from 48.2% to 66.9%, whereas the fraction of cells in the S phase decreased from 23.9% to 7.4%; however, the fraction of cells in the G2/M phase was not affected after treatment.

3.6. Gene expression profile

After analyzing the cytotoxic and apoptosis inducing effects of the flavopiridol, we are evaluated the gene expression profiles of

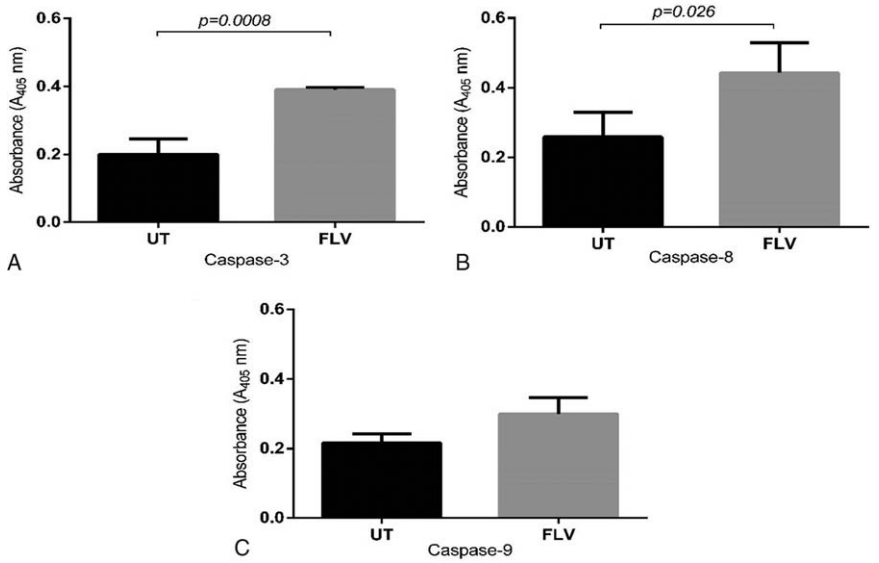

Figure 2. Caspase-3, caspase-8, and caspase-9 activities in untreated and flavopiridol-treated CD133^{high}/CD44^{high} lung CSCs. Cells were treated with 676.3 nM flavopiridol for 48 h. Caspase-3, -8, and -9 activities were analyzed using Colorimetric Assay Kits. (A) Caspase-3, (B) Caspase-8, (C) Caspase-9. Caspase-3 and caspase-8 activities significantly increased following treatment of flavopiridol, which was applied to cells at the IC_{50} dose. Data were representative of 1 of 3 similar experiments. CSCs = cancer stem cells.

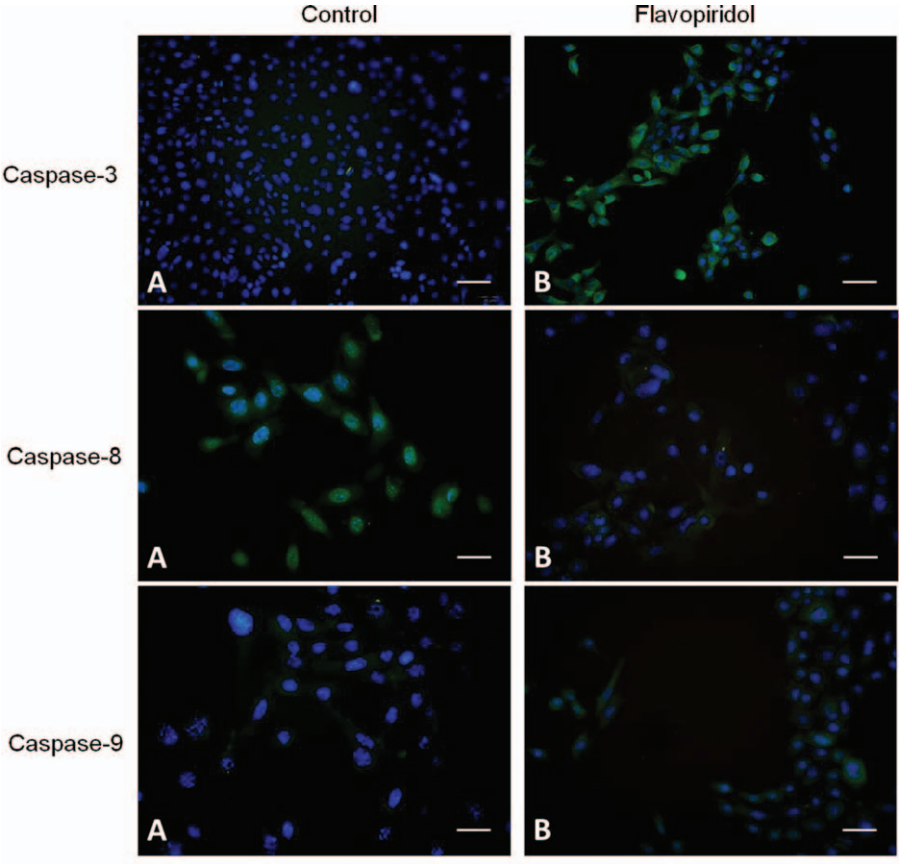

Figure 3. Immunofluorescence staining of caspase-3, caspase-8, and caspase-9 in CD133^{high}/CD44^{high} lung CSCs following treatment of the half maximal inhibitory concentration (IC_{50}) value of the flavopiridol. (A) Control (untreated group). (B) Flavopiridol-treated group. Immunofluorescence staining of caspase-3, caspase-8, and caspase-9 was visualized using FITC-conjugated secondary antibody (green). Nuclear staining was visualized using DAPI (4',6-diamidino-2-phenylindole) (blue) staining. Images are representative of 3 independent experiments. CSCs = cancer stem cells, FITC = fluorescein isothiocyanate.

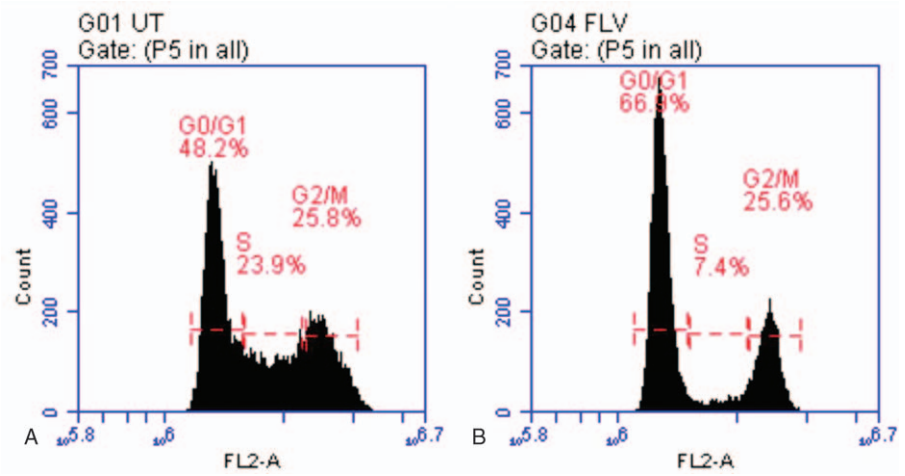

Figure 4. Cell cycle profiles obtained by flow cytometry (propidium iodide staining). (A) Control (untreated control cells) (UT). (B) Cells treated with 676 nM flavopiridol for 48 h (FLV). Notably, flavopiridol significantly influenced cell cycle arrest in the G0/G1 phase.

control and flavopiridol-treated $CD133^{high}/CD44^{high}$ lung CSCs focusing on the cell cytoskeleton, cell polarity, cell motility, cell cycle, and apoptosis. Hierarchical clustering of the control and flavopiridol-treated groups is shown in Fig. 5. As shown in Table 1, which summarized significantly increased or decreased genes compared to control, we observed very intense changes in the mRNA expressions of the genes that regulate cell cytoskeleton in terms of actin, tubulin, and cytokeratin. LIM domain kinase-1 (Limk1) which is a serine/threonine kinase that regulates actin polymerization via phosphorylation and inactivation of the actin binding factor cofilin and plays a role in many cellular processes associated with cytoskeletal structure. We found that flavopiridol treatment caused 16.77-fold decrease in the Limk1 gene expression ($P=1.60E-09$). Crk mRNA expression also decreased significantly after flavopiridol treatment. Formin-binding protein-1-like (Fnbp1l) was the third gene associated with actin polymerization and decreased 13.40 fold in flavopiridol-treated $CD133^{high}/CD44^{high}$ lung CSCs ($P=1.60E-09$). Slingshot protein phosphatase-1 (Ssh1), ArfGAP with RhoGAP domain, ankyrin repeat and PH domain-1 (Arap1) and p21 protein -Cdc42/Rac-activated kinase-4 (Pak4) were the most significantly decreased genes (−16.14 fold, $P=1.60E-09$; −14.53 fold, $P=2.10E-09$; −10.84 fold, $P=1.60E-09$ respectively) that regulate actin cytoskeleton, cell polarity, and motility. Furthermore, keratin 18 (Krt18) and Krt7 expressions exhibited −18.48 fold ($P=$ 1.60E-09) and −9.00fold ($P=2.25E-09$) decrease in the flavopiridol-treated group. Gene expressions analyses of cell cycle regulator genes revealed that Cyclin-dependent kinase -2 (Cdk2) inhibited significantly (−75.86 fold, $P=1.60E-09$) and Cdkn1a (p21), Chek2, Cdc25a, and Cdc25c were the other most decreased genes in the flavopiridol-treated $CD133^{high}/CD44^{high}$ lung CSCs. Additionally, expression of antiapoptotic protein B-cell CLL/lymphoma-2 (Bcl2) gene decreased 33.46-fold in the flavopiridol-treated cells and confirmed us apoptosis inducing effects of flavopiridol.

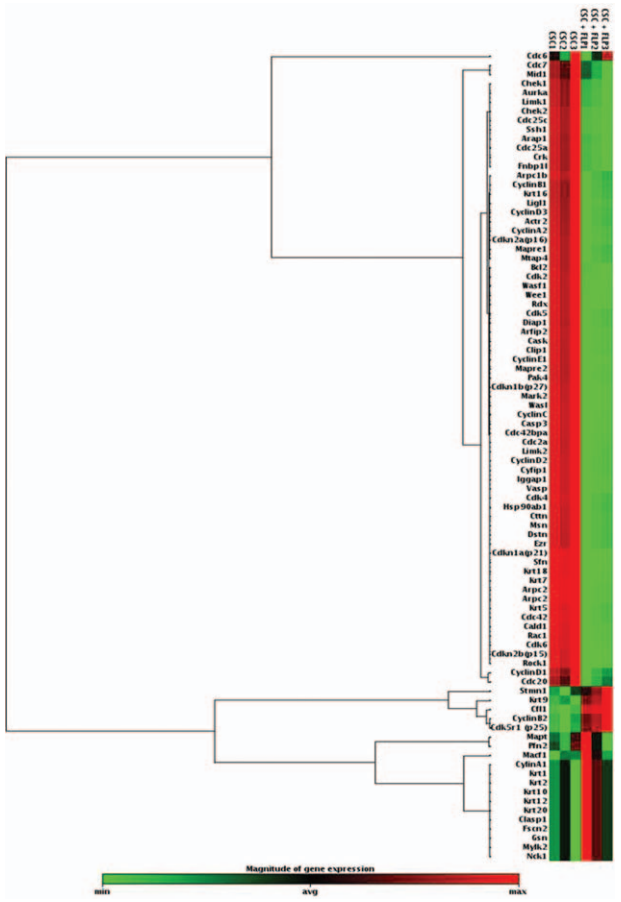

Figure 5. Hierarchical clustering of the lung CSCs and flavopiridol treated CSCs. Each sample was performed in triplicate. A pseudo color scale bar represented the fold change relative to the mean of the data for each RNA. CSCs = cancer stem cells.

3.7. Expression of e-cadherin, hsp90β, actin, tubulin, occludin, and CK2 in CSCs

Immunofluorescence staining was used to detect the expression of e-cadherin, hsp90β, actin, tubulin, occludin, and CK2 in $CD133^{high}/CD44^{high}$ lung CSCs following treatment of the half maximal inhibitory concentration (IC_{50}) value of the flavopiridol. We found that the level of e-cadherin, hsp90β, actin, and CK2 were markedly decreased in cells treated with flavopiridol (Fig. 6). There was no significant tubulin immunoreactivity in flavopiridol-treated group when compared to the untreated

Table 1

Comparison of significant gene expression differences between CSCs and flavopiridol treated CSCs.

Function	Gene symbol	CSC means	CSC+FLP means	Fold change	*P*ue
Actin cytoskeleton	Crk	0.00003	0.000002	−16.07	1.60E-09
	Fnbp1l	0.0003	0.00002	−13.40	1.60E-09
	Iggap1	0.020	0.002	−8.16	6.81E-09
	Limk1	0.0002	0.00001	−16.77	1.60E-09
	Limk2	0.010	0.003	−3.41	8.10E-09
Actin cytoskeleton, cell adhesion, cell motility	Msn	0.030	0.010	−3.00	5.31E-08
Actin cytoskeleton, cell motility	Arpc2	0.170	0.030	−5,67	5.91E-09
Actin cytoskeleton, cell motility/migration	Cald1	0.050	0.009	−5,59	4.99E-09
	Dstn	0.030	0.010	−3.00	2.99E-08
	Rac1	0.040	0.009	−4.57	7.29E-09
Actin cytoskeleton, cell polarity	Arap1	0.0003	0.00002	−14.53	2.10E-09
	Cdc42	0.170	0.070	−2.43	8.28E-08
	Cyfip1	0.020	0.006	−3.50	1.26E-08
Actin cytoskeleton, cell shape, size, polarity,	Ssh1	0.001	0.00003	−16.14	1.60E-09
Cell cytoskeleton, adhesion	Cttn	0.020	0.008	−2.48	2.99E-08
Cell cytoskeleton, cell motility, migration	Pak4	0.001	0.0001	−10.84	1.60E-09
Cell cytoskeleton, cell polarity, cell adhesion	Ezr	0.020	0.007	−2.72	6.86E-08
Cell motility/migration	Cdk5r1 (p25)	0.0002	0.0004	1.94	1.69E-07
Cell polarity	Ligl1	0.0003	0.00008	−4.19	9.32E-09
Cytokeratin	Krt16	0.001	0.0002	−2.93	3.65E-08
	Krt18	0.080	0.004	−18.48	1.60E-09
	Krt7	0.180	0.020	−9.00	2.25E-09
	Krt9	0.00002	0.0001	5.20	7.29E-09
Apoptosis	Bcl2	0.001	0.00003	−33.46	1.60E-09
Cell cycle	Cdc25a	0.0004	0.00002	−20.75	1.71E-09
	Cdc25c	0.001	0.00005	−11.74	2.32E-09
	Cdk2	0.002	0.00002	−75.86	1.60E-09
	Cdk4	0.080	0.040	−2.00	1.48E-07
	Cdkn1a (p21)	0.090	0.003	−33.83	1.60E-09
	Cdkn2a (p16)	0.002	0.0003	−4.76	8.10E-09
	Chek1	0.0002	0.00004	−4.31	9.32E-09
	Chek2	0.0005	0.00002	−28.44	1.60E-09
	CyclinA2	0.001	0.0001	−4.53	6.83E-09
	CyclinB1	0.001	0.0004	−2.44	6.53E-08
	CyclinD2	0.030	0.008	−3.55	1.26E-08
Cell cycle, microtubules	Aurka	0.0002	0.00005	−4.85	8.10E-09
Epithelial cell growth, cell cycle inhibition	Sfn	0.120	0.006	−19.14	1.71E-09

group. Immunofluorescence staining of occludin significantly increased following treatment of flavopiridol.

3.8. The percentages of $CD133^{high}/CD44^{high}$ cells in the flavopiridol-treated cells

In order to evaluate the relative percentage of $CD133^{high}/CD44^{high}$ cells following exposure to flavopiridol, cells were labeled with CD133 and CD44. Flow cytometric analysis showed that the percentages of $CD133^{high}/CD44^{high}$ cells showed significant changes when compared to the untreated cells (Fig. 7). After the flavopiridol treatment, lung CSCs maintained a lower fraction of $CD133^{high}/CD44^{high}$ cells (1.3%) compared with that (8%) in the control untreated cells.

4. Discussion

Cell polarization, cell motility, cell cytoskeleton, and epithelial \mesenchymal transition play a critical role on oncogenesis, differentiation of cell, and formation of cell hierarchy. There is a significant void in cancer biology with regard to the elucidation of the mechanisms that underlie tumor formation and progression. Recently, the existence of a hierarchy within cancer cell populations has been demonstrated experimentally for several tumor types. The identification of a tumor cell subset that is capable of self-renewal and, concurrently, generation into more differentiated progeny has engendered new perspectives toward selective targeting of tumors. Although the identification of the so-called cancer stem cells is a leap in the study of cancer ontogenesis, therapeutic targeting of such cells is plagued by significant difficulties. The current study aimed to investigate the effects of flavopiridol on lung squamous cancer stem cell.

Tumors contain a minority population of cells within tumors is responsible for tumor initiation, growth, resistance to the conventional treatments. Therefore, attention has been focused on defining new anticancer drug for cancer prevention and therapy by eliminating CSCs. For cancer prevention and treatment, we need to identify and characterize CSCs. CSCs have been isolated and identified using specific markers such as CD44, CD133, CD24, $\alpha 2\beta 1$ integrin, and aldehyde dehydrogenase1 (ALDH1). For lung cancer stem cell isolation, CD133 and CD44 were widely used as surface markers.[13,14] The same surface markers for the cancer stem cell were used in our study.

Apoptosis is one of the most critical and well-studied mechanisms, governing tissue development and homeostasis through a complex network of molecules that mediate death and

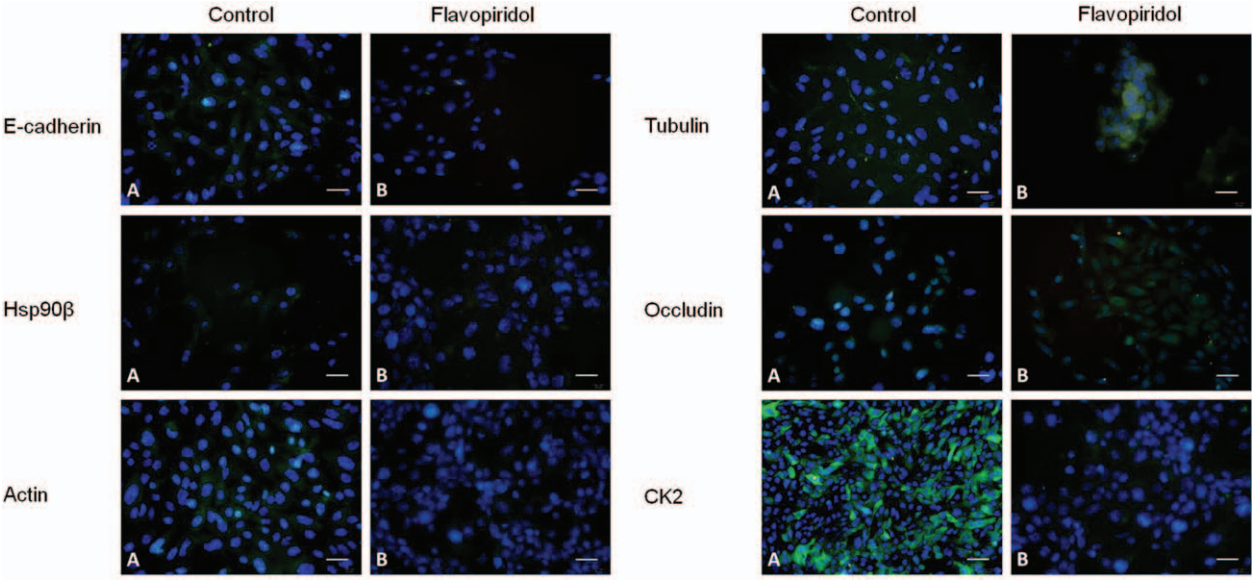

Figure 6. Immunofluorescence staining of e-cadherin, hsp90β, actin, tubulin, occludin, CK2 in CD133^{high}/CD44^{high} lung CSCs following treatment of the half maximal inhibitory concentration (IC_{50}) value of the flavopiridol. (A) Control (untreated group). (B) Flavopiridol-treated group. Nuclear staining was visualized using DAPI (4′,6–diamidino–2–phenylindole) (blue) staining. Images are representative of 3 independent experiments. CSCs = cancer stem cells.

survival signals. Escape from such a finely tuned death program is a prerequisite for any tumor-initiating cell. Thus, many compounds have been developed to target cancer cells and induce apoptosis directly or indirectly.[15] Accumulating evidence suggests that the resistance of CSCs to many conventional therapies accounts for the inability of these therapies to cure cancers.[16] Several potential mechanisms that influence cancer resistance to conventional therapy are being examined, but therapeutic interventions still face significant hurdles. A large body of experimental evidence suggests that CSCs have evolved strategies to evade cell death that is induced by radio- and chemo-therapeutic treatments. Several mechanisms have been proposed to govern CSC resistance, including impaired apoptotic machinery, increased DNA damage repair following radio- and chemotherapy, altered cell cycle checkpoint control, and upregulation of multidrug resistance to proteins.[15]

Defects in apoptosis can result in the expansion of a population of neoplastic cells and because the death of tumor cells by chemotherapy and radiotherapy is mediated largely by the activation of apoptosis, deregulation of apoptosis will render tumor cells resistant to antitumor treatments. CSCs have many of the prerequisites for a tumor cell to be resistant to treatments and reconstitute the bulk tumor mass. Our result has been shown that flavopiridol induces apoptotic pathway through caspases activation and a decrease in Bcl-2 expression in CSCs. In most tumors, antiapoptotic Bcl-2 family members are overexpressed in

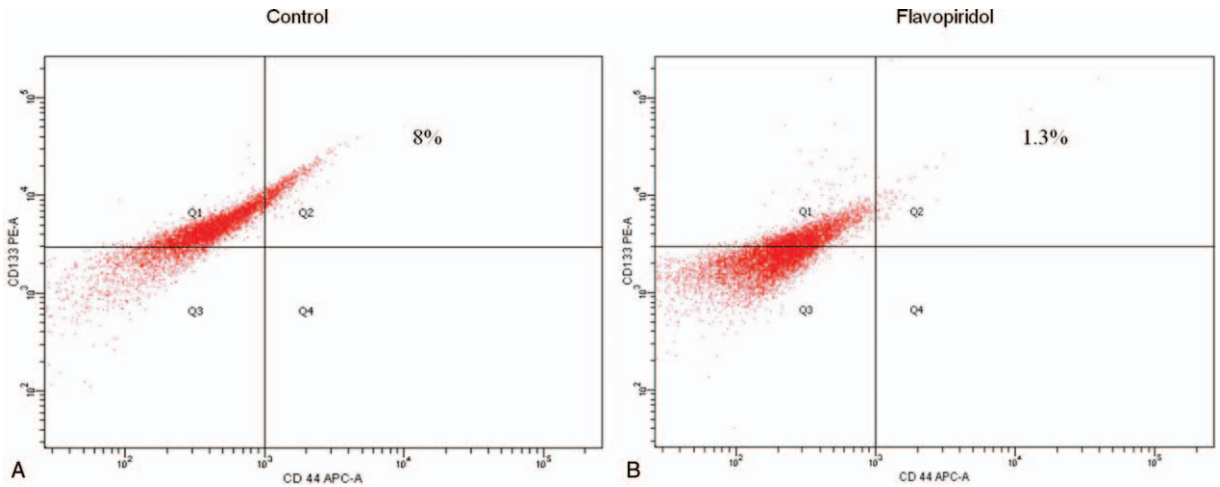

Figure 7. Flow cytometric analysis of CD133 and CD44 expression in CD133^{high}/CD44^{high} lung CSCs 48 h after flavopiridol treatment. (A) Control (untreated group). (B) Flavopiridol treated group. Expression profiles of CD133 and CD44 and their coexpression in CD133^{high}/CD44^{high} lung CSCs were examined. Suspensions cells were labeled with PE-conjugated anti-CD133 and FITC-conjugated anti-CD44 antibodies. The percentage of CD133 and CD44 at 48 h following drug treatment was assessed by flow cytometric analysis. The percentages of CD133^{high} and CD44^{high} cells showed significant decrease following treatment of flavopiridol. Data were calculated from 3 independent experiments. CSCs = cancer stem cells.

CSCs.[17] It has been reported that flavopiridol downregulates bcl–2 mRNA and protein expression.[18] Additionally, flavopiridol suppressed the cell cycle components and led to the reorganization of the cell cycle. Cell cycle defects in human cancers are associated with Cdks activity and their inhibition can lead to both cell cycle arrest and apoptosis. It was shown that flavopiridol induces G1 arrest through inhibition of Cdk. This compound has previously been shown to produce a block in cell cycle progression at the G1 phase.[19] Both normal and cancer stem cells have the ability to divide symmetrically, creating 2 identical daughter cells. They also have the ability to divide asymmetrically, forming 1 stem cell and 1 progenitor cell, the latter of which will undergo differentiation.[20] This asymmetric division facilitates healthy growth in normal cells due to the polarity involved in cell division. When this polarity is lost, the stem cells multiply and form a tumor.[20] Cell polarity plays an important role in many biological process, such as cell adhesion, migration, cell division, and EMT.[21] Loss of polarity by overexpression of polarity proteins leads to tumor invasion and metastasis.[22] G-proteins, such as RhoA, Cdc42, play an important role in cell polarity establishment and maintenance.[23] Targeting cell polarity proteins by flavopiridol may represent a new interesting approach to stop tumor progression.

Stem cell self-renewal is controlled by both intercellular mechanisms, via signaling from neighboring cells, and intracellular mechanisms, involving differential gene expression that is under epigenetic, transcriptional, translational, and post translational control.[24] Cytoskeleton parameters are effective structures on the cell division pattern. Therefore, in our study, these components were investigated in CSCs and after the administration of flavopiridol. The results showed that flavopiridol has a significant effect on the cytoskeletal components.

EMT programs were first observed in the context of embryonic development, such as gastrulation and neural crest formation.[25,26] Specifically, EMTs generate mesenchymal cell types from epithelial and endothelial precursors. These epithelial–mesenchymal conversions are crucial for cell movements that take place during morphogenesis, such as neural crest migration. This explains why the EMTs described in carcinoma cells have been portrayed as opportunistic activations of normally latent, early embryogenic cell-biological programs.[27]

CDK inhibitors participate in various cellular processes such as DNA repair, transcription, cell migration, cytoskeleton dynamics, and cell motility. According to previous studies, CDKs play a role in cancer cell invasion/migration and actin cytoskeleton regulation.[28,29] Our results showed that flavopiridol affected CSCs by regulating genes closely related to the cell cycle and actin cytoskeleton. Cyclins and CDK inhibitors involved in cell morphogenesis, adhesion, migration, and cytokinesis.[30] The changes within the organization of the actin cytoskeleton and cell motility allows metastatic cells to invade other tissues and organs. LIMK1/Pak4/Crk which play central roles in RhoGTPase regulation of the actin cytoskeleton involved in cell morphology and cell migration. It was reported that PAK4-LIMK1 pathway increased in cancer cell migration.[31] Our results showed that the expression levels of LIMK1/Pak4/Crk were decreased. Regarding this, it is believed that flavopiridol affected CSCs though reorganization of the actin cytoskeleton. EMT process can be regulated remodeling of the actin cytoskeleton dynamics, cell polarity and motility. The present study showed that flavopiridol changed the mRNA expressions of the genes that regulate cell cytoskeleton in terms of actin, tubulin, and cytokeratin. Taken together, these findings indicate that flavopiridol could play roles in EMT of CSCs.

CSCs exhibit a number of properties that would not seem to be directly connected to the trait of self-renewal, but might nonetheless be positively regulated by EMT-transcription factors. For example, Twist has been shown to directly suppress apoptosis through various mechanisms: by suppressing the pro-apoptotic effects of the Myc oncogene,[32] through activation of NF-kappa-β signaling, and by repression of p53-induced proapoptotic genes.[33,34] The resulting elevated resistance to apoptosis might well contribute to a crucial property of metastasizing CSCs by promoting carcinoma cell survival during early steps of metastasis and, following dissemination, during their attempts at gaining a foothold in distant, potentially in hospitable tissue microenvironments. A more attractive prospect comes from the discoveries that EMTs are induced by contextual signals, such as TGF-β, EGF, FGFs, Wnt and Notch ligands. In our own work, we find that signals of this sort are critically involved in both the initiation of EMT programs and the subsequent maintenance of cells in the resulting stem-cell state.[35] These signaling pathways have already been the objects of intensive drug development, largely because they play roles in the pathogenesis of a wide variety of diseases. In our study, the expression of EMT markers was studied in CSCs via E-cadherin and Occludin. The results demonstrated that Occludin expression significantly increased at the cellular level, whereas e-cadherin expression significantly decreased. Several studies have reported a conjunction between CSCs and EMT. EMT regulators play the critical role of EMT regulators in regulating CSC plasticity during tumor progression.[36] Recent studies also found that non-CSCs are populations that can generate CSCs de novo, and the CSC plasticity is controlled by the activation of EMT programs. CD133 has been shown to be related to the EMT program of head and neck carcinoma cells.[37] Also, it has been reported that $CD133^{+}$ cell population in primary nonsmall cell lung cancer have have greater tumorigenic potential, adhesion, and motility when compared to their $CD133^{-}$ counterparts.[38] In our study, flow cytometric analysis showed that the population of $CD133^{high}$ and $CD44^{high}$ significantly decreased after the flavopiridol treatment.

5. Conclusion

In our study, it was clear that flavopiridol significantly decreased the mRNA expressions of the genes that regulate the cell cytoskeleton and cell cycle components and cell motility in CSCs. E-cadherin, which plays an important role of EMT, significantly decreased with flavopridol therapy of $CD133^{high}/CD44^{high}$ lung CSCs. Flavopiridol also provided a significant reduction in the population of $CD133^{high}$ and $CD44^{high}$ lung CSCs. The concept of CSCs might have profound implications for our understanding of tumor biology and for the development of novel treatments that target them to eradicate tumors.

References

[1] Jemal A, Siegel R, Ward E, et al. Cancer statistics. CA Cancer J Clin 2008;58:71–96.
[2] Meyerson M, Carbone D. Genomic and proteomic profiling of lung cancers: lung cancer classification in the age of targeted therapy. J Clin Oncol 2005;23:3219–26.
[3] Lapidot T, Sirard C, Vormoor J, et al. A cell initiating human acute myeloid leukaemia after transplantation into SCID mice. Nature 1994;367:645–8.
[4] Eramo A, Lotti F, Sette G, et al. Identification and expansion of the tumorigenic lung cancer stem cell population. Cell Death Differ 2008;15:504–14.

[5] Beck B, Blanpain C. Unravelling cancer stem cell potential. Nat Rev Cancer 2013;13:727–38.
[6] Tan AR, Swain SM. Review of flavopiridol, a cyclin-dependent kinase inhibitor, as breast cancer therapy. Semin Oncol 2002;29:77–85.
[7] Newcomb EW, Tamasdan C, Entzminger Y, et al. Flavopiridol induces mitochondrial–mediated apoptosis in murine glioma GL261 cells via release of cytochrome c and apoptosis inducing factor. Cell Cycle 2003;2:243–50.
[8] Hugo H, Ackland ML, Blick T, et al. Epithelial–mesenchymal and mesenchymal–epithelial transitions in carcinoma progression. J Cell Physiol 2007;213:374–83.
[9] Dow LE, Brumby AM, Muratore R, et al. hScrib is a functional homologue of the Drosophila tumour suppressor Scribble. Oncogene 2003;22:9225–30.
[10] Liu Y, Chen LP. The regulation of cell polarity in the progression of lung cancer. J Cancer Res Ther 2013;2:S80–5.
[11] Danial NN, Korsmeyer SJ. Cell death: critical control points. Cell 2004;116:205–19.
[12] He YC, Zhou FL, Shen Y, et al. Apoptotic death of cancer stem cells for cancer therapy. Int J Mol Sci 2014;15:8335–51.
[13] Bertolini G, Roz L, Perego P, et al. Highly tumorigenic lung cancer CD133 + cells display stem-like features and are spared by cisplatin treatment. Proc Natl Acad Sci USA 2009;106:16281–6.
[14] Leung EL, Fiscus RR, Tung JW, et al. Non-small cell lung cancer cells expressing CD44 are enriched for stem cell-like properties. PLoS One 2010;5:e14062.
[15] Signore M, Ricci-Vitiani L, De Maria R. Ratgeting apoptosis pathway in cancer stem cell. Cancer Lett 2013;332:374–82.
[16] Medina V, Calvo MB, Diaz-Prado S, et al. Hedgehog signalling as a target in cancer stem cells. Clin Transl Oncol 2009;11:199–207.
[17] Madjd Z, Mehrjerdi AZ, Sharifi AM, et al. CD44+ cancer cells express higher levels of the anti-apoptotic protein Bcl-2 in breast tumours. Cancer Immun 2009;9:4.
[18] König A, Schwartz GK, Mohammad RM, et al. The novel cyclin-dependent kinase inhibitor flavopiridol downregulates Bcl–2 and induces growth arrest and apoptosis in chronic B–cell leukemia lines. Blood 1997;90:4307–12.
[19] Kaur G, Stetler-Stevenson M, Sehers S, et al. Growth inhibition with reversible cell cycle arrest of carcinoma cells by flavone L86-8275. J Nail Cancer Inst 1992;84:1736–40.
[20] Morrison SJ, Kimble J. Asymmetric and symmetric stem-cell divisions in development and cancer. Nature 2006;441:1068–74.
[21] Asnacios A, Hamant O. The mechanics behind cell polarity. Trends Cell Biol 2012;22:584–91.
[22] Muthuswamy SK, Xue B. Cell polarity as a regulator of cancer cell behavior plasticity. Annu Rev Cell Dev Biol 2012;28:599–625.
[23] Iden S, Collard JG. Crosstalk between small GTPases and polarity proteins in cell polarization. Nat Rev Mol Cell Biol 2008;9:846–59.
[24] Lin H. The stem-cell niche theory: lessons from flies. Nat Rev Genet 2002;3:931–40.
[25] Shook D, Keller R. Mechanisms, mechanics and function of epithelial–mesenchymal transitions in early development. Mech Dev 2003;120:1351–83.
[26] Nieto MA. The ins and outs of the epithelial to mesenchymal transition in health and disease. Annu Rev Cell Dev Biol 2011;27:347–76.
[27] Acloque H, Adams MS, Fishwick K, et al. Epithelial–mesenchymal transitions: the importance of changing cell state in development and disease. J Clin Invest 2009;119:1438–49.
[28] Song Y, Zhao C, Dong L, et al. Overexpression of cyclin B1 in human esophageal squamous cell carcinoma cells induces tumor cell invasive growth and metastasis. Carcinogenesis 2008;29:307–15.
[29] Zhong Z, Yeow WS, Zou C, et al. Cyclin D1/cyclindependent kinase 4 interacts with filamin A and affects the migration and invasion potential of breast cancer cells. Cancer Res 2010;70:2105–14.
[30] Bendris N, Lemmers B, Blanchard JM. Cell cycle, cytoskeleton dynamics and beyond: the many functions of cyclins and CDK inhibitors. Cell Cycle 2015;14:1786–98.
[31] Ahmed T, Shea K, Masters JR, et al. A PAK4-LIMK1 pathway drives prostate cancer cell migration downstream of HGF. Cell Signal 2008;20:1320–8.
[32] Valsesia-Wittmann S, Magdeleine M, Dupasquier S, et al. Oncogenic cooperation between H-Twist and N-Myc overrides failsafe programs in cancer cells. Cancer Cell 2004;6:625–30.
[33] Maestro R, Dei Tos AP, Hamamori Y, et al. Twist is a potential oncogene that inhibits apoptosis. Genes Dev 1999;13:2207–17.
[34] Pham CG, Bubici C, Zazzeroni F, et al. Upregulation of Twist-1 by NF-kappaB blocks cytotoxicity induced by chemotherapeutic drugs. Mol Cell Biol 2007;27:3920–35.
[35] Gupta PB, Onder TT, Jiang G, et al. Identification of selective inhibitors of cancer stem cells by high-throughput screening. Cell 2009;138: 645–59.
[36] Chaffer CL, Brueckmann I, Scheel C, et al. Normal and neoplastic nonstem cells can spontaneously convert to a stem-like state. Proc Natl Acad Sci USA 2011;108:7950–5.
[37] Chen YS, Wu MJ, Huang CY, et al. CD133/Src axis mediates tumor initiating property and epithelial mesenchymal transition of head and neck cancer. PLoS One 2011;6:e28053.
[38] Bertolini G, Roz L, Perego P, et al. Highly tumorigenic lung cancer CD133+ cells display stem-like features and are spared by cisplatin treatment. Proc Natl Acad Sci USA 2009;106:16281–6.